Innovative integration technologies for Kaup-Newell model: sub-picosecond optical pulses in birefringent fibers

Bahadır Kopçasız[1] and Fatma Nur Kaya Sağlam[2]

[1]Bursa Uludag Universitesi Fen Edebiyat Fakultesi
[2]Tekirdag Namik Kemal Universitesi Matematik Bolumu

August 24, 2024

Abstract

This research deals with the Kaup-Newell model (KNM), a class of nonlinear Schrödinger equations with important applications in plasma physics and nonlinear optics. Soliton solutions are essential for analyzing nonlinear wave behaviors in different physical systems, and the KNM is also significant in this context. The model's ability to represent sub-picosecond pulses makes it a significant tool for the research of nonlinear optics and plasma physics. Overall, the KNM is an important research domain in these areas, with ongoing efforts focused on understanding its various solutions and potential applications. A new version of the generalized exponential rational function method (nGERFM) and (G ' G 2) -expansion function methods are utilized to discover diverse soliton solutions. The nGERFM facilitates the generation of multiple solution types, including singular, shock, singular periodic, exponential, combo trigonometric, and hyperbolic solutions in mixed forms. Thanks to (G ' G 2) -expansion function method, we obtain trigonometric, hyperbolic, and rational solutions. The modulation instability (MI) of the proposed model is examined, with numerical simulations complementing the analytical results to provide a better understanding of the solutions' dynamic behavior. These results offer a foundation for future research, making the solutions effective, manageable, and reliable for tackling complex nonlinear problems. The methodologies used in this study are robust, influential, and practicable for diverse nonlinear partial differential equations (NLPDEs); to our knowledge, for this equation, these methods of investigation have not been explored before. The accuracy of each solution has been verified using the Maple software program.

Innovative integration technologies for Kaup-Newell model: sub-picosecond optical pulses in birefringent fibers

Bahadır Kopçasız[1,*] and Fatma Nur Kaya Sağlam[2]
[1]Department of Mathematics, Faculty of Arts and Sciences,
Bursa Uludag University, 16059 Bursa, Turkey

[2]Department of Mathematics, Faculty of Arts and Science,
Tekirdağ Namık Kemal University, 59030 Tekirdağ, Turkey

* Corresponding author e-mail:bkopcasz@gmail.com

July 14, 2024

Abstract

This research deals with the Kaup-Newell model (KNM), a class of nonlinear Schrödinger equations with important applications in plasma physics and nonlinear optics. Soliton solutions are essential for analyzing nonlinear wave behaviors in different physical systems, and the KNM is also significant in this context. The model's ability to represent sub-picosecond pulses makes it a significant tool for the research of nonlinear optics and plasma physics. Overall, the KNM is an important research domain in these areas, with ongoing efforts focused on understanding its various solutions and potential applications. A new version of the generalized exponential rational function method (nGERFM) and $\left(\frac{G'}{G^2}\right)$-expansion function methods are utilized to discover diverse soliton solutions. The nGERFM facilitates the generation of multiple solution types, including singular, shock, singular periodic, exponential, combo trigonometric, and hyperbolic solutions in mixed forms. Thanks to $\left(\frac{G'}{G^2}\right)$-expansion function method, we obtain trigonometric, hyperbolic, and rational solutions. The modulation instability (MI) of the proposed model is examined, with numerical simulations complementing the analytical results to provide a better understanding of the solutions' dynamic behavior. These results offer a foundation for future research, making the solutions effective, manageable, and reliable for tackling complex nonlinear problems. The methodologies used in this study are robust, influential, and practicable for diverse nonlinear partial differential equations (NLPDEs); to our knowledge, for this equation, these methods of investigation have not been explored before. The accuracy of each solution has been verified using the Maple software program.

1 Introduction

The advancement of many scientific and engineering fields has been greatly supported by nonlinear partial differential equations (NLPDEs), which provide valuable insights into the complexities of

physical and biological processes. The historical development of NLPDEs dates back to the 18th and 19th century, when mathematicians and physicists first began to formulate mathematical models to describe natural phenomena. Initially emerging in the study of fluid dynamics, heat transfer, and wave propagation, these equations have since found applications in a wide array of disciplines, including electrical engineering, magnetism, quantum mechanics, and biological systems. Over time, the study and solution of NLPDEs have evolved, driven by both theoretical advancements and the increasing power of computational methods, leading to a deeper understanding and more accurate modeling of intricate systems [1–4].

In the 19th century, Scottish engineer John Scott Russell first observed solitons, which are extraordinary nonlinear wave phenomena that sustain their shape while propagating at a uniform speed. He noticed a solitary wave that traveled long distances without dissipating, a phenomenon that intrigued scientists for decades. The mathematical foundation of solitons was later developed in the 1960s with the advent of the Korteweg-de Vries (KdV) equation, which describes shallow water waves. Solitons have since found applications across various fields, including fiber optic communications, where they enable stable, long-distance data transmission; plasma physics, where they help explain phenomena in magnetic fields; and even in biological systems, such as in the propagation of nerve impulses. The study of solitons has not only deepened our understanding of nonlinear wave dynamics but also spurred technological innovations in multiple domains [5–9].

Analytical solutions to NLPDEs provide profound insights into the behavior of complex systems governed by these equations. Unlike their linear counterparts, NLPDEs often exhibit intricate and diverse phenomena such as shock waves, solitons, and turbulence, making their solutions highly valuable but challenging to obtain. Analytical methods aim to find the exact solutions or simplifications that reveal the underlying structure and dynamics of the problem. Techniques such as the separation of variables, similarity transformations, the method of characteristics, and the inverse scattering transform has been developed to tackle specific types of NLPDEs. These methods not only help in understanding the fundamental properties of the solutions but also serve as benchmarks for validating numerical and approximate solutions. Despite their complexity, analytical solutions remain a cornerstone in the study of NLPDEs, offering clarity and depth to the exploration of nonlinear systems in physics, engineering, and beyond. In the present day, there are numerous trustworthy and well-developed techniques for finding both analytic and numerical solutions to NLPDEs, including the well-regarded modified auxiliary equation method [10], extended sinh-Gordon expansion technique [11], improved tanh approach [12], extended $\left(\frac{G'}{G^2}\right)$-expansion method [13], improved F-expansion method [14], polynomial expansion technique [15], Sumudu transform homotopy perturbation method (STHPM) [16], Painlevé analysis [17], Lie group analysis, group invariant solutions, and conservation laws [18], Hirota bilinear method [19] and so on.

In this work, we will examine the KNM, which is described by [20]:

$$i\frac{\partial \Gamma(x,t)}{\partial t} + \theta\frac{\partial^2 \Gamma(x,t)}{\partial x^2} + i\alpha\frac{\partial}{\partial x}\left(|\Gamma(x,t)|^2\,\Gamma(x,t)\right) - i\beta\frac{\partial}{\partial x}\left(|\Gamma(x,t)|^2\right)\Gamma(x,t) = 0, \tag{1}$$

in which $i^2 = -1$, $\Gamma = \Gamma(x,t)$ represents a complex-valued wave function. The specific meanings of the non-zero real coefficients θ, α, and β represent coefficient of group velocity dispersion, coefficient of self-steepening term and coefficient of nonlinear dispersion, respectively.

This study emphasizes the need for innovative solution methods to uncover the fundamental mathematical frameworks governing real-world physical systems. We present efficient analytical techniques based on finite series expansion to generate new and exact wave solutions for the KNM,

revealing results that have not been documented before. These techniques serve as powerful tools for researchers addressing challenging mathematical issues in various scientific areas.

The principal aim of this study is to investigate different and novel optical soliton solutions for Eq.(1). In this sense, the nGERFM and the $\left(\frac{G'}{G^2}\right)$-expansion function method will be used. It can be easily concluded that these analytical solution methods are very effective and successful in finding exact solutions to NLPDEs.

The paper is structured as follows: Section 3 describes the techniques, specifically the nGERFM and $\left(\frac{G'}{G^2}\right)$-expansion function method. Analytical solutions for the model are discussed in Section 4. Section 5 offers comparisons, Section 6 presents graphical explanations and Section 7 explains the conclusions.

2 Methodology

Consider the NLPDE as follows:

$$Y_1[\Gamma(x,t), \frac{\partial}{\partial t}\Gamma(x,t), \frac{\partial}{\partial x}\Gamma(x,t), \frac{\partial^2}{\partial t^2}\Gamma(x,t), \frac{\partial^2}{\partial x^2}\Gamma(x,t), ...] = 0. \tag{2}$$

By implementing the complex wave transformation shown below

$$\Gamma(x,t) = \Phi(\xi)\exp(i\tau(x,t)), \quad \xi = x - \omega t, \quad \tau(x,t) = -sx + ct + c_0, \tag{3}$$

Eq.(2) is transferred to

$$Y_2[\Phi, \Phi', \Phi'', \Phi''', ...] = 0. \tag{4}$$

In Eq.(3), ω, s and c are the non-zero real constants.

2.1 The details of the nGERFM

Step 1. Let we set up the solution of Eq.(4) as [21]:

$$\Phi(\xi) = k_0 + \sum_{n=1}^{n_0} k_n \left(\frac{\daleth'(\xi)}{\daleth(\xi)}\right)^n + \sum_{n=1}^{n_0} l_n \left(\frac{\daleth'(\xi)}{\daleth(\xi)}\right)^{-n}, \tag{5}$$

in which

$$\daleth(\xi) = \frac{\varsigma_1 \exp(\jmath_1\xi) + \varsigma_2 \exp(\jmath_2\xi)}{\varsigma_3 \exp(\jmath_3\xi) + \varsigma_4 \exp(\jmath_4\xi)}. \tag{6}$$

In the pre-assumed structures Eq.(6) and Eq.(5), $\varsigma_i, \jmath_i$ $(i \in [1,4])$ and k_0, k_n, l_n $(n \in [1, n_0])$ are unknown coefficients. In addition, to determine the value of the positive integer n_0, we can make use of various balancing rules documented in the literature.

Step 2. Substituting the expression from Eq.(5) into Eq.(4) produces a polynomial equation $\Pi(\varrho_1, \varrho_2, \varrho_3, \varrho_4) = 0$ in terms of $\varrho_n = e^{(\jmath_v\xi)}$ for $v = 1, 2, 3, 4$.

Step 3. At last, we obtain analytical solutions for Eq.(2) by substituting the results derived from solving this system into the general expression of Eq.(5).

2.2 The summary of $\left(\frac{G'}{G^2}\right)$-expansion function method

Step 1. Consider the solution of Eq.(4) is characterized by the expression in $\left(\frac{G'}{G^2}\right)$-expansion method as follows [22]:

$$\Phi(\xi) = \rho_0 + \sum_{n=1}^{n_0} \left(\rho_n \left(\frac{G'}{G^2}\right)^n + \sigma_n \left(\frac{G'}{G^2}\right)^{-n} \right), \tag{7}$$

in which $G = G(\xi)$ holds

$$\left(\frac{G'}{G^2}\right)' = \mu + \lambda \left(\frac{G'}{G^2}\right)^2, \tag{8}$$

where $\lambda \neq 0$, $\mu \neq 1$ are integers. To complete the process, it is necessary to find the constants ρ_0, ρ_n, σ_n $(n = 1, 2, 3, ..., n_0)$.

Step 2. As a result, $\left(\frac{G'}{G^2}\right)$ provides the following three types of solutions:

Scenario I, Trigonometric family: If $\mu\lambda > 0$, then

$$\left(\frac{G'}{G^2}\right) = \sqrt{\frac{\mu}{\lambda}} \left(\frac{\Theta_1 \cos\left(\sqrt{\mu\lambda}\xi\right) + \Theta_2 \sin\left(\sqrt{\mu\lambda}\xi\right)}{\Theta_2 \cos\left(\sqrt{\mu\lambda}\xi\right) - \Theta_1 \sin\left(\sqrt{\mu\lambda}\xi\right)} \right). \tag{9}$$

Scenario II, Hyperbolic family: When $\mu\lambda < 0$, then

$$\left(\frac{G'}{G^2}\right) = -\frac{\sqrt{|\mu\lambda|}}{\lambda} \left(\frac{\Theta_1 \sinh\left(2\sqrt{|\mu\lambda|}\xi\right) + \Theta_1 \cosh\left(2\sqrt{|\mu\lambda|}\xi\right) + \Theta_2}{\Theta_1 \sinh\left(2\sqrt{|\mu\lambda|}\xi\right) + \Theta_1 \cosh\left(2\sqrt{|\mu\lambda|}\xi\right) - \Theta_2} \right). \tag{10}$$

Scenario III, Rational family: When $\mu = 0$, $\lambda \neq 0$, then

$$\left(\frac{G'}{G^2}\right) = \left(-\frac{\Theta_1}{\lambda\left(\Theta_1\xi + \Theta_2\right)} \right), \tag{11}$$

in which Θ_1 and Θ_2 are constants.

Step 3. To find the n_0, the homogeneous balance rule is applied.

Step 4. By inserting from equations Eq.(7) and Eq.(8) into Eq.(4), we get a set of algebraic equations.

Step 5. By investigating the specific terms, we found the necessary set of parameters.

3 Extraction of the soliton solutions

The real and imaginary parts of Eq.(1) can be obtained by adopting Eq.(3):

$$\theta\Phi'' - (c + \theta s^2)\Phi + \alpha s \Phi^3 = 0, \tag{12}$$

and

$$-(\omega - 2\theta s)\Phi' + (3\alpha - 2\beta)\Phi^2\Phi' = 0. \tag{13}$$

From Eq.(13), we can establish the following constraint conditions:

$$\alpha = \frac{2}{3}\beta \tag{14}$$

with the speed of soliton:

$$\omega = 2\theta s. \tag{15}$$

Utilizing Eq.(14) into Eq.(12) yields

$$\theta\Phi'' - (c + \theta s^2)\Phi + \frac{2}{3}s\beta\Phi^3 = 0. \tag{16}$$

$3n_0 = n_0 + 2$ is obtained by using certain standard balancing principles in Eq.(16) between Φ^3 and Φ''. Hence, one should take $n_0 = 1$.

3.1 Main results of solving model Eq.(1) using technique I

Eq.(5) can be expressed as

$$\Phi(\xi) = k_0 + k_1\left(\frac{\daleth'(\xi)}{\daleth(\xi)}\right) + l_1\left(\frac{\daleth'(\xi)}{\daleth(\xi)}\right)^{-1}. \tag{17}$$

$\daleth(\xi)$ is specified by Eq.(6).

Class 1:

Taking $[\varsigma_1, \varsigma_2, \varsigma_3, \varsigma_4] = [1, 1, 1, 0]$ and $[\jmath_1, \jmath_2, \jmath_3, \jmath_4] = [0, 1, 2, 0]$ in Eq.(6) yields

$$\daleth(\xi) = \frac{1 + \exp(\xi)}{\exp(2\xi)}. \tag{18}$$

To obtain the parameter values, we solve the algebraic equations with Maple (or Mathematica). The collection of responses generated might be given as:

Type 1.1:

$$c = -\frac{\theta}{2}\left(2s^2 + 1\right),$$

$$k_0 = \mp\frac{5}{2}\sqrt{-\frac{3\theta}{\beta s}}, \qquad k_1 = \pm\sqrt{-\frac{3\theta}{\beta s}}, \qquad l_1 = 0.$$

By plugging the aforementioned values of k_0, k_1, l_1 into Eq.(17), we get

$$\Phi^{\pm}(\xi) = \frac{\sqrt{3}}{2}\sqrt{-\frac{\theta}{\beta s}} \times \left(\frac{\exp(\xi) - 1}{\exp(\xi) + 1}\right). \tag{19}$$

We find the following exponential function solution for Eq.(1) using Eq.(19)

$$\Gamma^{\pm}_{1,1}(x,t) = \frac{\sqrt{3}}{2}\sqrt{-\frac{\theta}{\beta s}} \times \left(\frac{\exp(x - \omega t) - 1}{\exp(x - \omega t) + 1}\right) \times \exp(i\left\{-sx + ct + c_0\right\}). \tag{20}$$

Type 1.2:

$$c = -\frac{\theta}{2}\left(2s^2+1\right),$$

$$k_0 = \mp\frac{5}{2}\sqrt{-\frac{3\theta}{\beta s}}, \qquad k_1 = 0, \qquad l_1 = \pm 6\sqrt{-\frac{3\theta}{\beta s}}.$$

By inserting the aforementioned values of k_0, k_1, l_1 into Eq.(17), we get

$$\Phi^{\mp}(\xi) = -\frac{\sqrt{3}}{2}\sqrt{-\frac{\theta}{\beta s}} \times \left(\frac{3\exp(\xi)-2}{3\exp(\xi)+2}\right). \tag{21}$$

The exponential function solution for Eq.(1) is found using Eq.(21) in the following manner:

$$\Gamma^{\mp}_{1,2}(x,t) = -\frac{\sqrt{3}}{2}\sqrt{-\frac{\theta}{\beta s}} \times \left(\frac{3\exp(x-\omega t)-2}{3\exp(x-\omega t)+2}\right) \times \exp(i\left\{-sx+ct+c_0\right\}). \tag{22}$$

Class 2:
When we pick $[\varsigma_1, \varsigma_2, \varsigma_3, \varsigma_4] = [1, -1, 2i, 0]$ and $[\jmath_1, \jmath_2, \jmath_3, \jmath_4] = [i, -i, 1, 0]$ in Eq.(6), we reach

$$\urcorner(\xi) = \frac{\sin(\xi)}{\exp(\xi)}. \tag{23}$$

To acquire parameter values, we use package programs to solve algebraic equations; the collection of solutions that result can be stated as:
Type 2.1:

$$c = -\theta(s^2-2),$$

$$k_0 = \pm\sqrt{-\frac{3\theta}{\beta s}}, \qquad k_1 = 0, \qquad l_1 = \pm 2\sqrt{-\frac{3\theta}{\beta s}}.$$

These values are entered into Eq.(17), yielding

$$\Phi^{\pm}(\xi) = \sqrt{3}\sqrt{-\frac{\theta}{\beta s}} \times \left(\frac{\sin(\xi)+\cos(\xi)}{\cos(\xi)-\sin(\xi)}\right). \tag{24}$$

By employing Eq.(24), we derive the following combo trigonometric soliton solution for Eq.(1):

$$\Gamma^{\pm}_{2,1}(x,t) = \sqrt{-\frac{3\theta}{\beta s}} \times \left(\frac{\cos(x-\omega t)+\sin(x-\omega t)}{\cos(x-\omega t)-\sin(x-\omega t)}\right) \times \exp(i\left\{-sx+ct+c_0\right\}). \tag{25}$$

Type 2.2:

$$c = -\theta(s^2-2),$$

$$k_0 = \mp \frac{3\theta}{\beta s \sqrt{-\frac{3\theta}{\beta s}}}, \qquad k_1 = \sqrt{-\frac{3\theta}{\beta s}}, \qquad l_1 = 0$$

These values are entered into Eq.(17), yielding

$$\Phi^{\pm}(\xi) = \sqrt{3}\sqrt{-\frac{\theta}{\beta s}} \times \cot(\xi). \tag{26}$$

By substituting Eq.(26), we derive the singular periodic solution for Eq.(1) as follows:

$$\Gamma^{\pm}_{2,2}(x,t) = \sqrt{3}\sqrt{-\frac{\theta}{\beta s}} \times \cot(x - \omega t) \times \exp(i\{-sx + ct + c_0\}). \tag{27}$$

Class 3:
For $[\varsigma_1, \varsigma_2, \varsigma_3, \varsigma_4] = [1, -1, 2, 0]$ and $[\jmath_1, \jmath_2, \jmath_3, \jmath_4] = [1, -1, -1, 0]$ in Eq.(6) provides

$$\urcorner(\xi) = \frac{\sinh(\xi)}{\exp(-\xi)}. \tag{28}$$

By implementing **the nGERFM** procedure, we obtain

$$c = -\theta\left(s^2 + 2\right),$$

$$k_0 = \mp \frac{3\theta}{\beta s \sqrt{-\frac{3\theta}{\beta s}}}, \quad k_1 = \pm\sqrt{-\frac{3\theta}{\beta s}}, \qquad l_1 = 0.$$

These values are entered into Eq.(17), yielding

$$\Phi^{\pm}(\xi) = \frac{\theta\sqrt{3}}{\beta s \sqrt{-\frac{\theta}{\beta s}}} \times \tanh(\xi). \tag{29}$$

By using Eq.(29), we reach the next shock solution for Eq.(1)

$$\Gamma^{\pm}_{3}(x,t) = \frac{\theta\sqrt{3}}{\beta s \sqrt{-\frac{\theta}{\beta s}}} \times \tanh(x - \omega t) \times \exp(i\{-sx + ct + c_0\}). \tag{30}$$

Class 4:
In Eq.(6), picking $[\varsigma_1, \varsigma_2, \varsigma_3, \varsigma_4] = [2, 0, 1, 1]$ and $[\jmath_1, \jmath_2, \jmath_3, \jmath_4] = [1, 0, i, -i]$ produces

$$\urcorner(\xi) = \frac{\exp(\xi)}{\cos(\xi)}. \tag{31}$$

We also achieve
Type 4.1:

$$c = -\theta\left(s^2 - 2\right),$$

$$k_0 = \pm\sqrt{-\frac{3\theta}{\beta s}}, \qquad k_1 = 0, \qquad l_1 = \mp 2\sqrt{-\frac{3\theta}{\beta s}}.$$

These findings combined with Eq.(17) produce

$$\Phi^{\pm}(\xi) = \sqrt{3}\sqrt{-\frac{\theta}{\beta s}} \times \left(\frac{2\cos(\xi)\sin(\xi) - 1}{2\cos(\xi)^2 - 1}\right). \tag{32}$$

As a result of our findings, the following combo trigonometric soliton solution is achieved:

$$\Gamma_{4,1}^{\pm}(x,t) = \sqrt{3}\sqrt{-\frac{\theta}{\beta s}} \times \left(\frac{2\cos(x-\omega t)\sin(x-\omega t) - 1}{2\cos(x-\omega t)^2 - 1}\right) \times \exp(i\{-sx + ct + c_0\}). \tag{33}$$

Type 4.2:

$$c = -\theta\left(s^2 - 2\right),$$

$$k_0 = \pm\frac{3\theta}{\beta s\sqrt{-\frac{3\theta}{\beta s}}}, \qquad k_1 = \pm\sqrt{-\frac{3\theta}{\beta s}}, \qquad l_1 = 0.$$

These findings combined with Eq.(17) yields

$$\Phi^{\mp}(\xi) = \frac{\theta\sqrt{3}}{\beta s\sqrt{-\frac{\theta}{\beta s}}} \times \tan(\xi). \tag{34}$$

Therefore, one way to describe the singular periodic solution is as

$$\Gamma_{4,1}^{\pm}(x,t) = \frac{\theta\sqrt{3}}{\beta s\sqrt{-\frac{\theta}{\beta s}}} \times \tan(x-\omega t) \times \exp(i\{-sx + ct + c_0\}). \tag{35}$$

Class 5:
In Eq.(6), considering $[\varsigma_1, \varsigma_2, \varsigma_3, \varsigma_4] = [2, 0, 1, 1]$ and $[\jmath_1, \jmath_2, \jmath_3, \jmath_4] = [0, 0, 1, -1]$ generates

$$\urcorner(\xi) = \frac{1}{\cosh(\xi)}. \tag{36}$$

We accomplish
Type 5.1:

$$c = -\theta\left(s^2 + 2\right),$$

$$k_0 = 0, \qquad k_1 = 0, \qquad l_1 = \pm\sqrt{-\frac{3\theta}{\beta s}}.$$

By plugging the values of k_0, k_1, l_1 into Eq.(17), we gain

$$\Phi^{\mp}(\xi) = \sqrt{3}\sqrt{-\frac{\theta}{\beta s}} \times \coth(\xi). \tag{37}$$

As a result, we can derive singular soliton solutions given by:

$$\Gamma_{5,1}^{\mp}(x,t) = \sqrt{3}\sqrt{-\frac{\theta}{\beta s}} \times \coth(x-\omega t) \times \exp(i\{-sx+ct+c_0\}). \tag{38}$$

Type 5.2:

$$c = -\theta\left(s^2+8\right),$$

$$k_0 = 0, \qquad k_1 = l_1 = \pm\sqrt{-\frac{3\theta}{\beta s}}.$$

For these reasons, along with Eq.(17), the following result is most likely to be achieved

$$\Phi^{\mp}(\xi) = \sqrt{3}\sqrt{-\frac{\theta}{\beta s}} \times \left(\frac{2\cosh(\xi)^2 - 1}{\cosh(\xi)\sinh(\xi)}\right). \tag{39}$$

The mixed form of the hyperbolic solution is expressed as

$$\Gamma_{5,2}^{\mp}(x,t) = \sqrt{3}\sqrt{-\frac{\theta}{\beta s}} \times \left(\frac{-1+2\cosh(x-\omega t)^2}{\sinh(x-\omega t)\cosh(x-\omega t)}\right) \times \exp(i\{-sx+ct+c_0\}). \tag{40}$$

Class 6:
In Eq.(6), considering $[\varsigma_1, \varsigma_2, \varsigma_3, \varsigma_4] = [2, 0, 1, 1]$ and $[\jmath_1, \jmath_2, \jmath_3, \jmath_4] = [-2, 0, 1, -1]$ generates

$$\urcorner(\xi) = \frac{\exp(-2\xi)}{\cosh(\xi)}. \tag{41}$$

We reach

$$c = -\theta\left(s^2+2\right),$$

$$k_0 = \pm 2\sqrt{-\frac{3\theta}{\beta s}}, \qquad k_1 = 0, \qquad l_1 = \pm 3\sqrt{-\frac{3\theta}{\beta s}}.$$

By entering the values of k_0, k_1, l_1 into Eq.(17), one gets

$$\Phi^{\pm}(\xi) = \sqrt{-\frac{1}{\rho}} \times \left(\frac{\cosh(\xi)+2\sinh(\xi)}{\sinh(\xi)+2\cosh(\xi)}\right). \tag{42}$$

We arrive at the combo soliton solution by using the Eq.(42)

$$\Gamma_{6}^{\pm}(x,t) = \sqrt{3}\sqrt{-\frac{\theta}{\beta s}} \times \left(\frac{2\sinh(x-\omega t)+\cosh(x-\omega t)}{2\cosh(x-\omega t)+\sinh(x-\omega t)}\right) \times \exp(i\{-sx+ct+c_0\}). \tag{43}$$

Class 7:
If we take $[\varsigma_1, \varsigma_2, \varsigma_3, \varsigma_4] = [1, 1, 2, 0]$ and $[\jmath_1, \jmath_2, \jmath_3, \jmath_4] = [i, -i, 0, 0]$ in Eq.(6) provides

$$\beth(\xi) = \cos(\xi). \tag{44}$$

We have,

$$c = -\theta\left(s^2 + 4\right),$$

$$k_0 = 0, \qquad k_1 = l_1 = \pm\sqrt{-\frac{3\theta}{\beta s}}.$$

When these results are analyzed in conjunction with Eq.(17), we get the following outcome

$$\Phi^{\mp}(\xi) = \sqrt{3}\sqrt{-\frac{\theta}{\beta s}} \times \frac{1}{\cos(\xi)\sin(\xi)}. \tag{45}$$

As a result, we have the periodic solution given below:

$$\Gamma_7^{\mp}(x,t) = \sqrt{3}\sqrt{-\frac{\theta}{\beta s}} \times \frac{1}{\cos(x-\omega t)\sin(x-\omega t)} \times \exp(i\{-sx + ct + c_0\}). \tag{46}$$

3.2 Main results of solving model Eq.(1) using technique II

Eq.(7) can be expressed as

$$\Phi(\xi) = \rho_0 + \rho_1\left(\frac{G'}{G^2}\right) + \sigma_1\left(\frac{G'}{G^2}\right)^{-1}, \tag{47}$$

in which ρ_0, ρ_1, and σ_1 are real parameters and are determined later. The use of Eq.(16) and Eq.(47) together with Eq.(8) gives the cluster of algebraic expression. By accumulating and equating to zero the power coefficients of the $\left(\frac{G'}{G^2}\right)$. The values of ρ_0, ρ_1, and σ_1 are derived by handling the resulting algebraic system.

Cluster 1: $c = -4\lambda\mu\theta - s^2\theta, \quad \rho_0 = 0, \quad \rho_1 = \pm\lambda\sqrt{-\frac{3\theta}{\beta s}}, \quad \sigma_1 = \pm\mu\sqrt{-\frac{3\theta}{\beta s}}.$

Cluster 2: $c = 2\lambda\mu\theta - s^2\theta, \quad \rho_0 = 0, \quad \rho_1 = \pm\lambda\sqrt{-\frac{3\theta}{\beta s}}, \quad \sigma_1 = 0.$

Cluster 3: $c = 2\lambda\mu\theta - s^2\theta, \quad \rho_0 = 0, \quad \rho_1 = 0, \quad \sigma_1 = \pm\mu\sqrt{-\frac{3\theta}{\beta s}}.$

For **Cluster 1,** the following solutions are built.

Case-1: If $\mu\lambda > 0$, then by using the Eq.(3), family of trigonometric solutions can be presented as follows:

$$\Gamma_{1,1}^{\pm}(x,t) = \left\{ \begin{array}{c} \frac{\lambda\sqrt{-\frac{3\theta}{\beta s}}\sqrt{\frac{\mu}{\lambda}}\left(\Theta_1\cos\left(\sqrt{\mu\lambda}(x-\omega t)\right)+\Theta_2\sin\left(\sqrt{\mu\lambda}(x-\omega t)\right)\right)}{\left(\Theta_2\cos\left(\sqrt{\mu\lambda}(x-\omega t)\right)-\Theta_1\sin\left(\sqrt{\mu\lambda}(x-\omega t)\right)\right)} \\ +\frac{\mu\sqrt{-\frac{3\theta}{\beta s}}\left(\Theta_2\cos\left(\sqrt{\mu\lambda}(x-\omega t)\right)-\Theta_1\sin\left(\sqrt{\mu\lambda}(x-\omega t)\right)\right)}{\sqrt{\frac{\mu}{\lambda}}\left(\Theta_1\cos\left(\sqrt{\mu\lambda}(x-\omega t)\right)+\Theta_2\sin\left(\sqrt{\mu\lambda}(x-\omega t)\right)\right)} \end{array} \right\} \times \exp(i\times\{-sx + ct + c_0\}). \tag{48}$$

Case-2: If $\mu\lambda < 0$, then by using the Eq.(3), family of hyperbolic solutions are written as follows:

$$\Gamma^{\pm}_{1,2}(x,t) = \left\{ \begin{array}{c} \frac{\lambda\sqrt{-\frac{3\theta}{\beta s}}\sqrt{-\frac{\mu}{\lambda}}\left(\Theta_1\cosh\left(2\sqrt{-\mu\lambda}(x-\omega t)\right)+\Theta_1\sinh\left(2\sqrt{-\mu\lambda}(x-\omega t)\right)+\Theta_2\right)}{\left(\Theta_1\cosh\left(2\sqrt{-\mu\lambda}(x-\omega t)\right)+\Theta_1\sinh\left(2\sqrt{-\mu\lambda}(x-\omega t)\right)-\Theta_2\right)} \\ -\frac{\mu\sqrt{-\frac{3\theta}{\beta s}}\left(\Theta_1\cosh\left(2\sqrt{-\mu\lambda}(x-\omega t)\right)+\Theta_1\sinh\left(2\sqrt{-\mu\lambda}(x-\omega t)\right)-\Theta_2\right)}{\sqrt{-\frac{\mu}{\lambda}}\left(\Theta_1\cosh\left(2\sqrt{-\mu\lambda}(x-\omega t)\right)+\Theta_1\sinh\left(2\sqrt{-\mu\lambda}(x-\omega t)\right)+\Theta_2\right)} \end{array} \right\} \times \exp(i\times\{-sx+ct+c_0\}). \tag{49}$$

Case-3: If $\mu = 0$, $\lambda \neq 0$, then by using the Eq.(3), a family of rational solutions are written as follows:

$$\Gamma^{\pm}_{1,3}(x,t) = \left\{ \frac{\sqrt{-\frac{3\theta}{\beta s}}\Theta_1}{\left(\Theta_1\left(x-\omega t\right)+\Theta_2\right)} - \frac{\lambda\mu\sqrt{-\frac{3\theta}{\beta s}}\left(\Theta_1\left(x-\omega t\right)+\Theta_2\right)}{\Theta_1} \right\} \times \exp(i\times\{-sx+ct+c_0\}). \tag{50}$$

For **Cluster 2,** the following solutions are built.

Case-1: If $\mu\lambda > 0$, then by using the Eq.(3), family of trigonometric solutions can be shown as follows:

$$\Gamma^{\pm}_{2,1}(x,t) = \left\{ \begin{array}{c} \frac{\lambda\sqrt{-\frac{3\theta}{\beta s}}\sqrt{\frac{\mu}{\lambda}}\left(\Theta_1\cos\left(\sqrt{\mu\lambda}(x-\omega t)\right)+\Theta_2\sin\left(\sqrt{\mu\lambda}(x-\omega t)\right)\right)}{\left(\Theta_2\cos\left(\sqrt{\mu\lambda}(x-\omega t)\right)-\Theta_1\sin\left(\sqrt{\mu\lambda}(x-\omega t)\right)\right)} \\ +\frac{\mu\sqrt{-\frac{3\theta}{\beta s}}\left(\Theta_2\cos\left(\sqrt{\mu\lambda}(x-\omega t)\right)-\Theta_1\sin\left(\sqrt{\mu\lambda}(x-\omega t)\right)\right)}{\sqrt{\frac{\mu}{\lambda}}\left(\Theta_1\cos\left(\sqrt{\mu\lambda}(x-\omega t)\right)+\Theta_2\sin\left(\sqrt{\mu\lambda}(x-\omega t)\right)\right)} \end{array} \right\} \times \exp(i\times\{-sx+ct+c_0\}). \tag{51}$$

Case-2: If $\mu\lambda < 0$, then by using the Eq.(3), family of hyperbolic solutions are written as follows:

$$\Gamma^{\pm}_{2.2}(x,t) = \left\{ \begin{array}{c} \frac{\lambda\sqrt{-\frac{3\theta}{\beta s}}\sqrt{-\frac{\mu}{\lambda}}\left(\Theta_1\cosh\left(2\sqrt{-\mu\lambda}(x-\omega t)\right)+\Theta_1\sinh\left(2\sqrt{-\mu\lambda}(x-\omega t)\right)+\Theta_2\right)}{\left(\Theta_1\cosh\left(2\sqrt{-\mu\lambda}(x-\omega t)\right)+\Theta_1\sinh\left(2\sqrt{-\mu\lambda}(x-\omega t)\right)-\Theta_2\right)} \\ -\frac{\mu\sqrt{-\frac{3\theta}{\beta s}}\left(\Theta_1\cosh\left(2\sqrt{-\mu\lambda}(x-\omega t)\right)+\Theta_1\sinh\left(2\sqrt{-\mu\lambda}(x-\omega t)\right)-\Theta_2\right)}{\sqrt{-\frac{\mu}{\lambda}}\left(\Theta_1\cosh\left(2\sqrt{-\mu\lambda}(x-\omega t)\right)+\Theta_1\sinh\left(2\sqrt{-\mu\lambda}(x-\omega t)\right)+\Theta_2\right)} \end{array} \right\} \times \exp(i\times\{-sx+ct+c_0\}). \tag{52}$$

Case-3: If $\mu = 0$, $\lambda \neq 0$, then by using the Eq.(3), a family of rational solutions are written as follows:

$$\Gamma^{\pm}_{2,3}(x,t) = \left\{ \frac{\sqrt{-\frac{3\theta}{\beta s}}\Theta_1}{\left(\Theta_1\left(x-\omega t\right)+\Theta_2\right)} - \frac{\lambda\mu\sqrt{-\frac{3\theta}{\beta s}}\left(\Theta_1\left(x-\omega t\right)+\Theta_2\right)}{\Theta_1} \right\} \times \exp(i\times\{-sx+ct+c_0\}). \tag{53}$$

For **Cluster 3,** the following solutions are built.

Case-1: If $\mu\lambda > 0$, then by using the Eq.(3), family of trigonometric solutions can be illustrated as follows:

$$\Gamma_{3,1}^{\pm}(x,t)=\left\{\begin{array}{c}\frac{\lambda\sqrt{-\frac{3\theta}{\beta s}}\sqrt{\frac{\mu}{\lambda}}\left(\Theta_1\cos\left(\sqrt{\mu\lambda}(x-\omega t)\right)+\Theta_2\sin\left(\sqrt{\mu\lambda}(x-\omega t)\right)\right)}{\left(\Theta_2\cos\left(\sqrt{\mu\lambda}(x-\omega t)\right)-\Theta_1\sin\left(\sqrt{\mu\lambda}(x-\omega t)\right)\right)}\\ +\frac{\mu\sqrt{-\frac{3\theta}{\beta s}}\left(\Theta_2\cos\left(\sqrt{\mu\lambda}(x-\omega t)\right)-\Theta_1\sin\left(\sqrt{\mu\lambda}(x-\omega t)\right)\right)}{\sqrt{\frac{\mu}{\lambda}}\left(\Theta_1\cos\left(\sqrt{\mu\lambda}(x-\omega t)\right)+\Theta_2\sin\left(\sqrt{\mu\lambda}(x-\omega t)\right)\right)}\end{array}\right\}\times\exp(i\times\{-sx+ct+c_0\}).\quad(54)$$

Case-2: If $\mu\lambda<0$, then by using the (3), family of hyperbolic solutions are written as follows:

$$\Gamma_{3,2}^{\pm}(x,t)=\left\{\begin{array}{c}\frac{\lambda\sqrt{-\frac{3\theta}{\beta s}}\sqrt{-\frac{\mu}{\lambda}}\left(\Theta_1\cosh\left(2\sqrt{-\mu\lambda}(x-\omega t)\right)+\Theta_1\sinh\left(2\sqrt{-\mu\lambda}(x-\omega t)\right)+\Theta_2\right)}{\left(\Theta_1\cosh\left(2\sqrt{-\mu\lambda}(x-\omega t)\right)+\Theta_1\sinh\left(2\sqrt{-\mu\lambda}(x-\omega t)\right)-\Theta_2\right)}\\ -\frac{\mu\sqrt{-\frac{3\theta}{\beta s}}\left(\Theta_1\cosh\left(2\sqrt{-\mu\lambda}(x-\omega t)\right)+\Theta_1\sinh\left(2\sqrt{-\mu\lambda}(x-\omega t)\right)-\Theta_2\right)}{\sqrt{-\frac{\mu}{\lambda}}\left(\Theta_1\cosh\left(2\sqrt{-\mu\lambda}(x-\omega t)\right)+\Theta_1\sinh\left(2\sqrt{-\mu\lambda}(x-\omega t)\right)+\Theta_2\right)}\end{array}\right\}\times\exp(i\times\{-sx+ct+c_0\}).\quad(55)$$

Case-3: If $\mu=0$, $\lambda\neq0$, then by using the Eq.(3), a family of rational solutions are written as follows:

$$\Gamma_{3,3}^{\pm}(x,t)=\left\{\frac{\sqrt{-\frac{3\theta}{\beta s}}\Theta_1}{\left(\Theta_1\left(x-\omega t\right)+\Theta_2\right)}-\frac{\lambda\mu\sqrt{-\frac{3\theta}{\beta s}}\left(\Theta_1\left(x-\omega t\right)+\Theta_2\right)}{\Theta_1}\right\}\times\exp(i\times\{-sx+ct+c_0\}).\quad(56)$$

4 Modulation instability analysis

In many nonlinear systems, the interplay between dispersive and nonlinear effects leads to modulation instability in steady states. Specifically, in the context of optical fibers, modulation instability is a well-researched phenomenon that is significant for designing fiber optic communication systems. Here, the optical signal propagates through the fiber and is represented by the wave field, with the Kerr effect causing nonlinearity by affecting the fiber's refractive index based on light intensity. In nonlinear wave equations, modulation instability describes how small perturbations can grow exponentially to form new structures or patterns. This section focuses on investigating the modulation instability (MI) of the equation using linear stability techniques. [23].

Eq.(1) provides a definition for the modulation instability of traveling waves. Assume that the perturbed solution is represented by

$$\Gamma\left(x,t\right)=\left(\sqrt{P}+u(x,t)\right)e^{i\lambda x},\quad(57)$$

in which λ is used to denote the normalized optical power. When we use Eq.(57) in Eq.(1), we obtain

$$iu_t-\theta\lambda^2u+2i\theta\lambda u_x+\theta u_{xx}=0.\quad(58)$$

Let us consider a solution to Eq.(58) expressed as

$$u(x,t)=l_1e^{i(kx-wt)}+l_2e^{-i(kx-wt)}.\quad(59)$$

Here, k is the normalized wave number and w denotes the frequency. By integrating Eq.(59) into Eq.(58), and isolating the coefficients of $e^{i(kx-wt)}$ and $e^{-i(kx-wt)}$ to solve the determinant of the coefficient matrix, we obtain the following dispersion relation:

$$\left(-\left(k-\lambda\right)^2\theta+w\right)-\left(k+\lambda\right)^2\theta-w=0. \tag{60}$$

By analyzing dispersion relation Eq.(60) for k, we can derive

$$k=\pm\frac{\sqrt{-\theta\left(\theta\lambda^2+w\right)}}{\theta}.$$

The dispersion relation obtained provides insights into the stability of the steady state. A real component for k indicates that the steady state is stable against small perturbations, whereas an imaginary k signifies instability and results in an exponential growth of perturbations.

5 Graphical Explanation

In this section, we will describe the parameters that were used to generate the plots. Using these parameters, we will illustrate 3D, contour, and density plots for some of the solutions that we have derived.

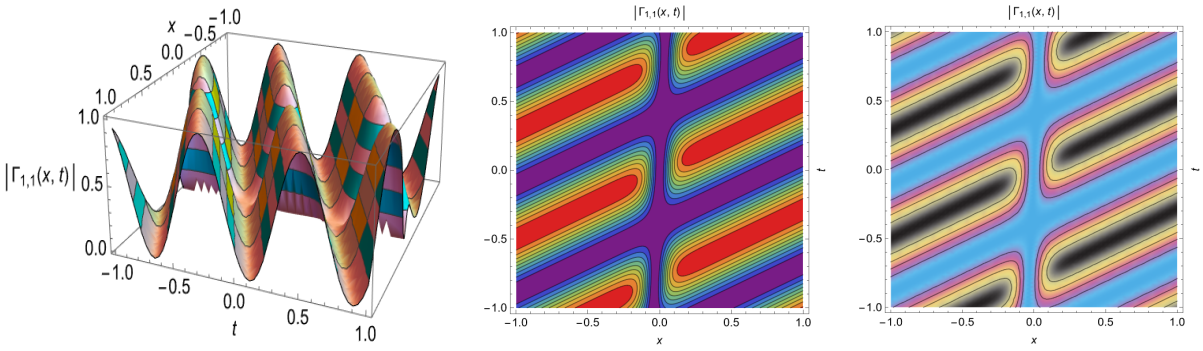

Figure 1. The 3D, contour, and density plots for the solution $|\Gamma_{1,1}(x,t)|$ in Eq.(20) when $\beta=3$, $\alpha=2$, $\theta=3$, $s=4$, $\omega=24$, $c=2$, $c_0=0$, and $\xi=x-\omega t$.

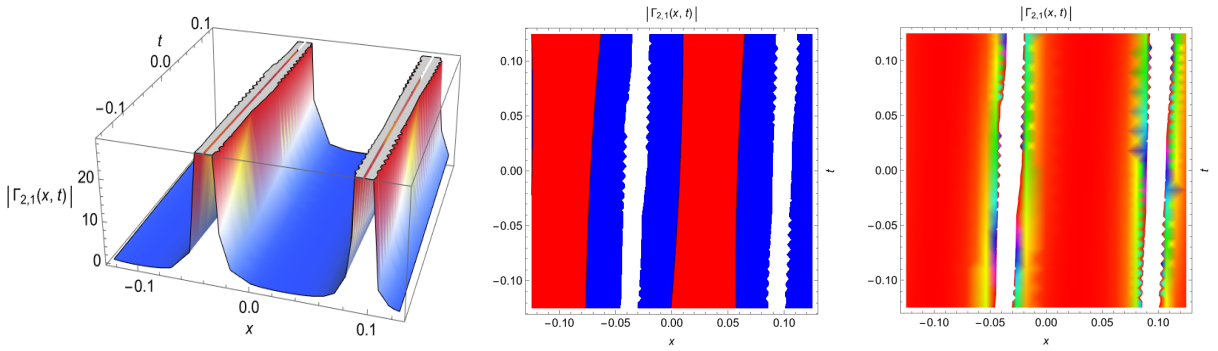

Figure 2. The 3D, contour, and density plots for the solution $|\Gamma_{2,1}(x,t)|$ in Eq.(25) when $\beta = 3$, $\alpha = 2$, $\theta = 3$, $s = 4$, $\omega = 24$, $c = 2$, $c_0 = 0$, and $\xi = x - \omega t$.

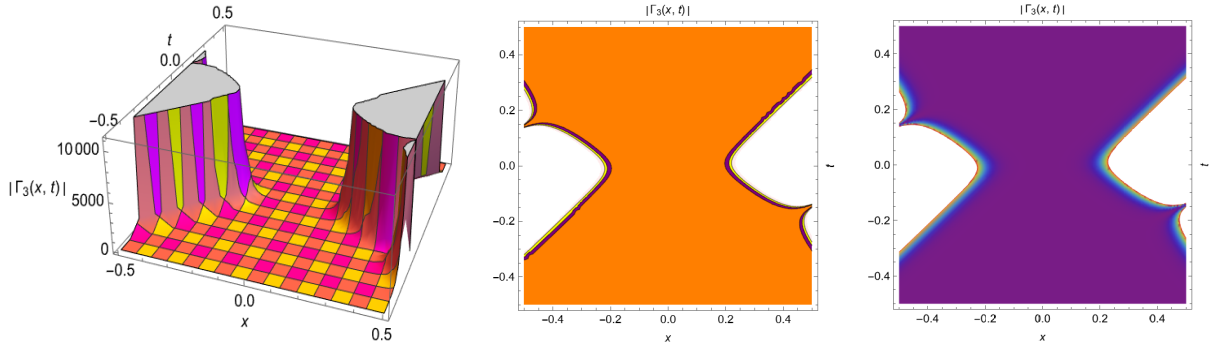

Figure 3. The 3D, contour, and density plots for the solution $|\Gamma_3(x,t)|$ in Eq.(30) when $\beta = 3$, $\alpha = 2$, $\theta = 3$, $s = 4$, $\omega = 24$, $c = 2$, $c_0 = 0$, and $\xi = x - \omega t$.

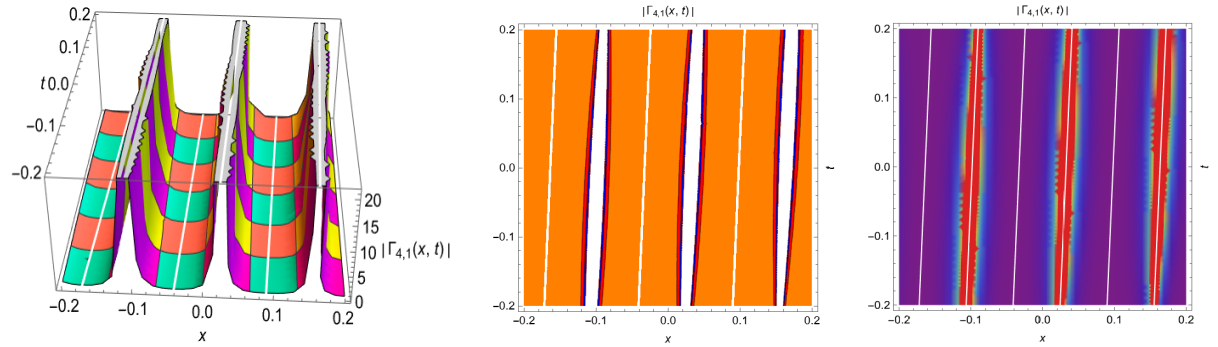

Figure 4. The 3D, contour, and density plots for the solution $|\Gamma_{4,1}(x,t)|$ in Eq.(33) when $\beta = 3$, $\alpha = 2$, $\theta = 3$, $s = 4$, $\omega = 24$, $c = 2$, $c_0 = 0$, and $\xi = x - \omega t$.

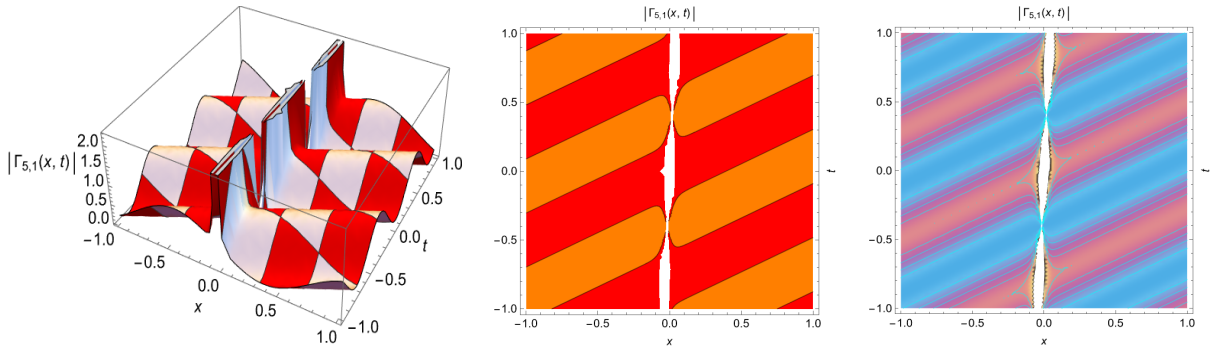

Figure 5. The 3D, contour, and density plots for the solution $|\Gamma_{5,1}(x,t)|$ in Eq.(38) when $\beta = 3$, $\alpha = 2$, $\theta = 3$, $s = 4$, $\omega = 24$, $c = 2$, $c_0 = 0$, and $\xi = x - \omega t$.

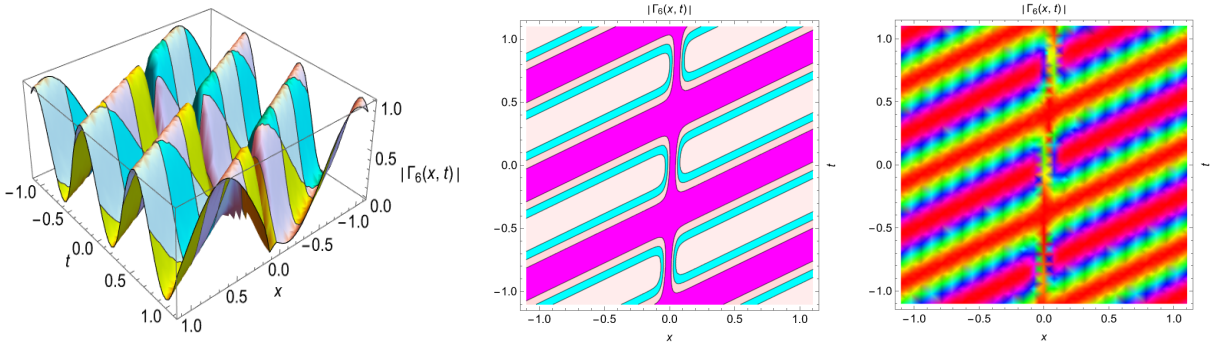

Figure 6. The 3D, contour, and density plots for the solution $|\Gamma_6(x,t)|$ in Eq.(43) when $\beta = 3$, $\alpha = 2$, $\theta = 3$, $s = 4$, $\omega = 24$, $c = 2$, $c_0 = 0$, and $\xi = x - \omega t$.

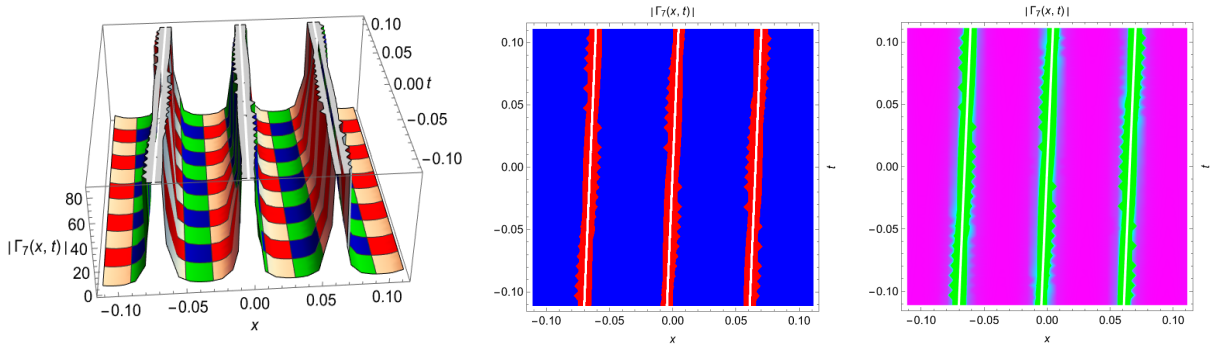

Figure 7. The 3D, contour, and density plots for the solution $|\Gamma_6(x,t)|$ in Eq.(46) when $\beta = 3$, $\alpha = 2$, $\theta = 3$, $s = 4$, $\omega = 24$, $c = 2$, $c_0 = 0$, and $\xi = x - \omega t$.

6 Comparisons

In this section, we compare the results of our investigation with those from previous studies that employed different analytical methods and are documented in the literature. Highlighting the unique qualities and innovative contributions of our present research is the aim of this comparative analysis. In [24], the KNM was studied by using the Jacobian elliptic function to find new type solutions. In [25], the author uncovered analytical solutions, including bright, dark, and singular solitons, and other types of solutions by using the extended simplest equation method. Our work synthesizes this research to apply the more effective technique, namely the nGERFM and $\left(\frac{G'}{G^2}\right)$-expansion function method. Thus, by implementing these two methods, we give novel soliton solutions, such as exponential function, singular periodic, shock, singular, combo trigonometric, hyperbolic solutions in mixed form, trigonometric, hyperbolic, and rational solutions.

As a result of carefully selecting the study's parameters, it becomes evident that many of the study's conclusions are in line with previous research findings. Recall that these outcomes were originally expressed differently from ours, even though there may have been some parallels. Despite an extensive search of relevant publications, no solution identical to the one revealed in this work could be found. The fact that the remaining results we have obtained do not seem to have been published before highlights their novelty and innovation. The outcomes displayed in this investigation were obtained by utilizing the nGERFM and $\left(\frac{G'}{G^2}\right)$-expansion function method.

7 Conclusion

In this study, the KNM models the glamorous technology of sub-picosecond pulses that spread via single-mode optical fibers is investigated using two innovative methods, namely the nGERFM and $\left(\frac{G'}{G^2}\right)$-expansion function method.

To begin with, we regarded the nGERFM. The use of nGERFM enabled us to obtain several classes of soliton solutions, such as shock, singular, singular periodic, exponential, combo trigonometric, and hyperbolic solutions in mixed forms. Secondly, we considered the $\left(\frac{G'}{G^2}\right)$-expansion function method. By using this method, we get trigonometric, hyperbolic, and rational soliton solutions. A key benefit of these techniques is their capability to predict and organize solution structures from the start. By using Mathematica to create 3D, density, and contour plots, we were able to graphically represent the obtained soliton solutions based on selected parameter values. The logical and lucid methodology makes it possible for interested parties to solve their NLPDEs right away. The outcomes of this research show that the offered methodology is promising for uncovering a variety of soliton solutions in nonlinear optical equations. The modulation instability (MI) analysis performed on the model also contributes new insights.

The soliton solutions we have achieved are original and unique to the KNM equation. Furthermore, in comparison to many previous studies, our discoveries offer a more exhaustive range of functions, including hyperbolic, periodic, rational, trigonometric, and exponential solutions. These validated solutions are applicable for analyzing NLPDEs across fields such as applied sciences, plasma physics, mathematical physics, nonlinear dynamics, and engineering. Future research could focus on examining the long-term behavior of these solitary wave solutions and exploring how different parameters affect system dynamics to discover new phenomena.

Funding There is no funding for this work.

Data availability All data generated or analyzed during this study are included in this published article.

Declarations

Conflict of interest The author declares that there is no conflict of interest regarding the research effort and the publication of this paper.

References

[1] Yaşar, E., Yıldırım, Y., & Adem, A. R. (2018). Perturbed optical solitons with spatio-temporal dispersion in (2+ 1)-dimensions by extended Kudryashov method. Optik, 158, 1-14.

[2] Çelik, N., Seadawy, A. R., Özkan, Y. S., & Yaşar, E. (2021). A model of solitary waves in a nonlinear elastic circular rod: abundant different type exact solutions and conservation laws. Chaos, Solitons & Fractals, 143, 110486.

[3] Seadawy, A. R., & Ali, A. (2023). Stability analysis and abundant closed-form wave solutions of the Date-Jimbo-Kashiwara-Miwa and combined sinh-cosh-Gordon equations arising in fluid mechanics. International Journal of Nonlinear Sciences and Numerical Simulation, 24(2), 791-810.

[4] Tang, L., Biswas, A., Yıldırım, Y., & Alshomrani, A. S. (2024). Bifurcations and optical soliton perturbation for the Lakshmanan–Porsezian–Daniel system with Kerr law of nonlinear refractive index. Journal of Optics, 1-6.

[5] Tipu, G. H., Faridi, W. A., Rizk, D., Myrzakulova, Z., Myrzakulov, R., & Akinyemi, L. (2024). The optical exact soliton solutions of Shynaray-IIA equation with Φ^6-model expansion approach. Optical and Quantum Electronics, 56(2), 226.

[6] Hossain, M. N., Alsharif, F., Miah, M. M., & Kanan, M. (2024). Abundant New Optical Soliton Solutions to the Biswas–Milovic Equation with Sensitivity Analysis for Optimization. Mathematics, 12(10), 1585.

[7] ur Rahman, M., Sun, M., Boulaaras, S., & Baleanu, D. (2024). Bifurcations, chaotic behavior, sensitivity analysis, and various soliton solutions for the extended nonlinear Schrödinger equation. Boundary Value Problems, 2024(1), 15.

[8] Younas, U., Yao, F., Nasreen, N., Khan, A., & Abdeljawad, T. (2024). On the dynamics of soliton solutions for the nonlinear fractional dynamical system: Application in ultrasound imaging. Results in Physics, 57, 107349.

[9] Khater, M. M. (2024). Modeling wave propagation with gravity and surface tension: Soliton solutions for the generalized hietarinta-type equation. Qualitative Theory of Dynamical Systems, 23(2), 86.

[10] Arshed, S., Akram, G., Sadaf, M., Nabi, A. U., & Alzaidi, A. S. (2024). Optical soliton solutions of perturbed nonlinear Schrödinger equation with parabolic law nonlinearity. Optical and Quantum Electronics, 56(1), 50.

[11] Raza, N., Jaradat, A., Basendwah, G. A., Batool, A., & Jaradat, M. M. M. (2024). Dynamic analysis and derivation of new optical soliton solutions for the modified complex Ginzburg-Landau model in communication systems. Alexandria Engineering Journal, 90, 197-207.

[12] Islam, M. T., Sarkar, T. R., Abdullah, F. A., & Gómez-Aguilar, J. F. (2024). Distinct optical soliton solutions to the fractional Hirota Maccari system through two separate strategies. Optik, 300, 171656.

[13] Khan, M. A. U., Akram, G., & Sadaf, M. (2024). Dynamics of novel exact soliton solutions of concatenation model using effective techniques. Optical and Quantum Electronics, 56(3), 385.

[14] Ahmad, J., Noor, K., Anwar, S., & Akram, S. (2024). Stability analysis and soliton solutions of truncated M-fractional Heisenberg ferromagnetic spin chain model via two analytical methods. Optical and Quantum Electronics, 56(1), 95.

[15] Adel, M., Tariq, K. U., Ahmad, H., & Kazmi, S. R. (2024). Soliton solutions, stability, and modulation instability of the (2+ 1)-dimensional nonlinear hyperbolic Schrödinger model. Optical and Quantum Electronics, 56(2), 182.

[16] Kapoor, M. (2024). A robust regime via Sumudu HPM for Schrödinger equation in different dimensions. Results in Optics, 14, 100619.

[17] Wazwaz, A. M. (2024). Extended (3+ 1)-dimensional Kairat-II and Kairat-X equations: Painlevé integrability, multiple soliton solutions, lump solutions, and breather wave solutions. International Journal of Numerical Methods for Heat & Fluid Flow, 34(5), 2177-2194.

[18] Kopçasız, B., & Yaşar, E. (2024). Dual-mode nonlinear Schrödinger equation (DMNLSE): Lie group analysis, group invariant solutions, and conservation laws. International Journal of Modern Physics B, 38(02), 2450020.

[19] Ma, Z., Wang, B., Liu, X., & Liu, Y. (2024). Bäcklund transformation, Lax pair and dynamic behaviour of exact solutions for a (3+ 1)-dimensional nonlinear equation. Pramana, 98(1), 24.

[20] Wang, K. J., Wang, G. D., & Shi, F. (2024). Sub-picosecond pulses in single-mode optical fibres with the Kaup–Newell model via two innovative methods. Pramana, 98(1), 26.

[21] Ghanbari, B., Baleanu, D.: Applications of two novel techniques in finding optical soliton solutions of modified nonlinear Schrödinger equations. Res. Phys. **44**, 106171 (2023)

[22] Bilal, M., Seadawy, A. R., Younis, M., Rizvi, S. T. R., & Zahed, H. (2021). Dispersive of propagation wave solutions to unidirectional shallow water wave Dullin–Gottwald–Holm system and modulation instability analysis. Mathematical Methods in the Applied Sciences, 44(5), 4094-4104.

[23] Ali, A., Ahmad, J., & Javed, S. (2023). Exact soliton solutions and stability analysis to (3+ 1)-dimensional nonlinear Schrödinger model. Alexandria Engineering Journal, 76, 747-756.

[24] Salas, A. H., El-Tantawy, S. A., & Youssef, A. A. A. R. (2020). New solutions for chirped optical solitons related to Kaup-Newell equation: Application to plasma physics. Optik, 218, 165203.

[25] Ahmed, H. M., Rabie, W. B., Arnous, A. H., & Wazwaz, A. M. (2020). Optical solitons in birefringent fibers of Kaup-Newell's equation with extended simplest equation method. Physica Scripta, 95(11), 115214.